THE JOURNAL OF PHYSICAL CHEMISTRY Letters

pubs.acs.org/JPCL

Evidence of Roaming Dynamics and Multiple Channels for Molecular Elimination in NO_3 Photolysis

Michael P. Grubb,[†] Michelle L. Warter,[†] Arthur G. Suits,[‡] and Simon W. North*[,†]

[†]Department of Chemistry, Texas A&M University, College Station, Texas 77842, and [‡]Department of Chemistry, Wayne State University, Detroit, Michigan 48202

ABSTRACT We report correlated state distributions arising from NO_3 photolysis at 588 nm using velocity map ion imaging. State-selected NO images reveal clear evidence for two dissociation pathways for the $NO + O_2$ channel. Vibrationally excited O_2 ($^3\Sigma_g^-$, v = 5−10) is formed in coincidence with low rotational states of NO ($^2\Pi$) in the dominant mechanism. We also observe a small channel consisting of low vibrational levels of O_2 ($^3\Sigma_g^-$, v = 0−4) coincident with high NO rotational states. We discuss the results in the context of the recent studies of formaldehyde dissociation and postulate the involvement of roaming-type dynamics.

SECTION Dynamics, Clusters, Excited States

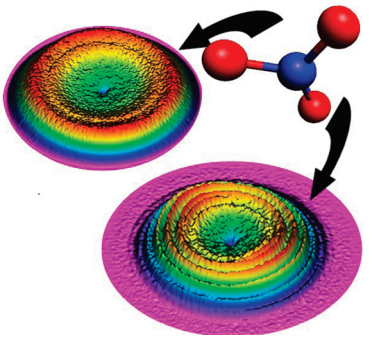

The nitrate radical, NO_3, plays an important role in atmospheric chemistry, photolyzing in the visible region to yield two product channels

$$NO_3 + h\nu \rightarrow NO + O_2 \quad (1)$$

$$\rightarrow NO_2 + O \quad (2)$$

The thresholds for both channels are close in energy (0.82 kcal/mol),[1] resulting in a narrow wavelength range (585−595 nm) for the molecular channel 1 since the higher-energy radical channel 2 dominates once it is energetically accessible.[2,3] The molecular channel threshold has been assumed to arise from a tight transition state involving a three-center mechanism.[4] However, no theoretical transition state of photochemically relevant energy has been identified to our knowledge, and the mechanism of molecular elimination remains unsolved.

There have been several experimental studies of NO_3 photodissociation. Total translational energy distributions obtained by Davis et al. revealed that O_2 from the molecular channel was highly excited, although it was unclear whether the energy was associated with electronic excitation ($^1\Delta_g$) or vibrational excitation (v = 5−10).[1] Interestingly, the translational energy distribution included a contribution at high energy corresponding to low internal energy states which did not exhibit well-resolved vibrational features. Correlated state distributions can often provide valuable insight into the underlying dynamics. Mikhaylichenko et al. measured correlated translational energy distributions in NO_3 photodissociation using pump−probe 1 +1 REMPI in a molecular beam, although the velocity resolution of the experiment was not sufficient to resolve individual O_2 vibrational states.[4] The state-selected NO translational energy distributions were consistent with the work of Davis et al.,[1] and the authors reported a nascent NO rotational temperature of 1400 ± 300 K.

We have obtained high-resolution state-selected NO translational energy distributions arising from NO_3 dissociation using velocity map ion imaging. Our results show clear state-dependent bimodal O_2 internal energy distributions, implying two distinct mechanisms in the dissociation. The results show an intriguing resemblance to the molecular elimination channel in formaldehyde photodissociation, in which one pathway evolves through a tight transition state and the second pathway "roams" over a large region of the potential energy surface before leading to intramolecular abstraction.[5] We speculate that a similar competition may be occurring in NO_3, although no conventional transition-state pathway has yet been identified for this system. This would be one of the first examples of roaming dynamics in an open-shelled system.[6] Additional theoretical and experimental studies aimed at resolving the mechanism of the NO + O_2 channel are currently underway.

Ion images of specific NO ($^2\Pi$) rotational states resulting from NO_3 dissociation at 588 nm were collected by state-selective ionization using a 1 +1 REMPI scheme. Figure 1 shows the raw (left) and reconstructed (right) images for NO ($^2\Pi_{3/2}$, v = 0, J = 6.5). Figure 2 shows the derived velocity distribution (symbols). The peaks correspond to different vibrational levels of the coincident O_2 molecule indicated in the comb in Figure 2. The solid line is a simulation using an assumed O_2 ($^3\Sigma_g^-$) vibrational distribution and a rotational temperature of 500 K. The simulation confirms that the low-velocity fragments arise from highly vibrationally excited O_2 ($^3\Sigma_g^-$), with minimal contribution from electronically excited O_2 ($^1\Delta_g$,$^1\Sigma_g^+$). Images associated with both spin−orbit states of NO were all found to be nearly identical. Measured signals observed from NO_3 dissociation were found to be isotropic, consistent with ground-state

Received Date: June 30, 2010
Accepted Date: July 26, 2010
Published on Web Date: July 28, 2010

DOI: 10.1021/jz1008888 | *J. Phys. Chem. Lett.* **2010**, *1*, 2455–2458

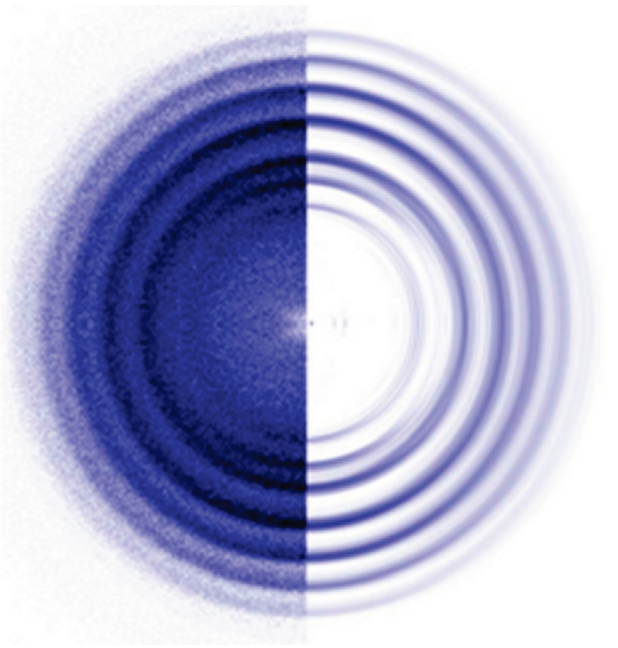

Figure 1. The raw (left) and reconstructed (right) ion image of NO ($^2\Pi$, N = 7) resulting from NO_3 photolysis at 588 nm.

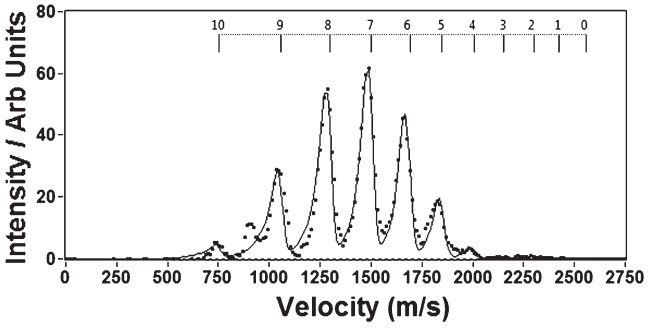

Figure 2. Velocity distribution derived from the data in Figure 1 (symbols). The solid line represents a simulated velocity distribution assuming an O_2 rotational temperature of 500 K. The O_2 vibrational state corresponding to each peak is indicated by the comb above the graph.

dissociation. The anisotropic signal in Figure 1 is due to NO_2 photodissociation at the probe wavelength and is seen in Figure 2 as the peak at 900 m/s. Figure 3 shows state-selected translational energy distributions derived from four NO rotational states, N = 13, 17, 21, and 26. The distributions clearly show evidence of bimodality with high O_2 vibrational state fragments correlated to low rotational states of NO and low O_2 vibrational states correlated to high NO rotational states. At NO (N = 7), the vibrationally excited O_2 (v = 4−10) makes up >99% of the total signal. Between NO (N = 7) and NO (N=17), vibrationally cold O_2 begins to appear (to about 10% of the signal at N = 17) and dominates the total signal at rotational states beyond N=26. At rotational states above N=33, the total signal decreases rapidly in accordance with the reported NO rotational temperature.[4] Our results also show a strong angular momentum correlation between the NO and O_2 fragments as evidenced by the broadening of the

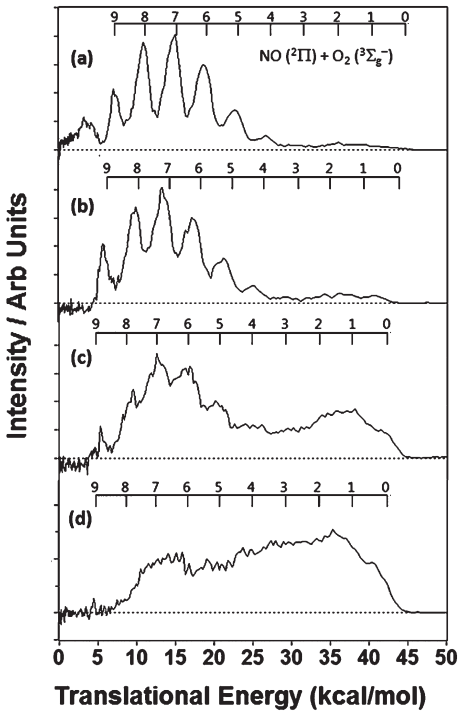

Figure 3. Total translational energy distributions associated with various rotational states of NO {N = 13 (a), 17 (b), 21 (c), and 26 (d)} resulting from NO_3 photolysis at 588 nm. The background signal has been removed by subtracting the probe-only contribution.

peak widths in the translational energy distributions shown in Figure 3. The simulated rotational temperature of the coincident O_2 ranges from approximately 500 K correlated to NO (N=7) to over 2000 K correlated with higher NO rotational states. We find that a Boltzmann-weighted sum of the translational energy distribution of each NO rotational state reproduces the total translational energy distribution of Davis et al.[1] (see also Supporting Information).

The bimodal energy distribution for the molecular elimination channel observed in NO_3 is similar to the distributions found in formaldehyde.[5] Elongated O_2 bond lengths associated with "early" abstraction by a roaming oxygen atom should result in the production of vibrationally excited O_2 from NO_3. It has recently been shown that product distributions resulting from a roaming mechanism should be similar to the product distributions resulting from a direct abstraction mechanism.[7] By analogy, roaming in NO_3 should yield similar product distributions to the $NO_2 + O(^3P) \rightarrow NO + O_2$ reaction. Smith et al. reported LIF measurements of the nascent vibrational distribution of the O_2 fragments arising from the thermal reaction of $NO_2 + O(^3P)$.[8] The authors observed that the O_2 vibrational populations decreased monotonically from v = 6 to 11. Their results are shown in Figure 4 and compared with the total O_2 vibrational distribution generated by a weighted sum of the correlated vibrational levels. Despite the lack of LIF data below v = 6 (due to diminishing Franck−Condon factors), the agreement between the two measurements is very good. We note that additional measurements of the $NO_2 + O(^3P)$ reaction which extend the detection of O_2 vibration to lower states would provide a stronger connection.

DOI: 10.1021/jz1008888 | J. Phys. Chem. Lett. 2010, 1, 2455–2458

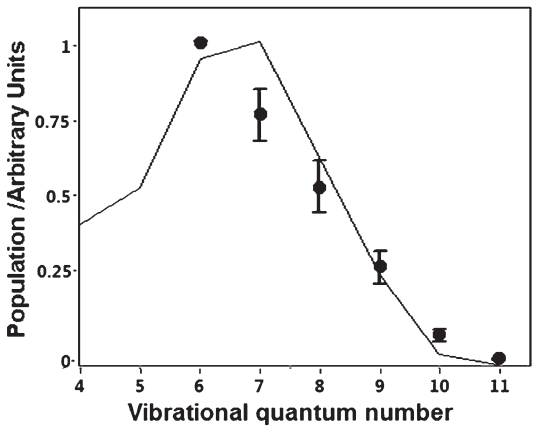

Figure 4. Total O_2 vibrational distribution from NO_3 dissociation (line) compared to the LIF measurements arising from the O (^{3}P) + $NO_2 \rightarrow NO + O_2$ reaction performed by Smith et al. (symbols).[8]

In addition, crossed beam experiments of the NO_2 + O (^{3}P) reaction would provide more direct insight into the nature of the abstraction mechanism involved in this system.

The relative yield of the roaming channel in formaldehyde, although varying with excitation wavelength, was always found to be less than 20% of the total product.[9] For NO_3 dissociation, if the vibrationally excited O_2 products are associated with a roaming mechanism, then this is the dominant pathway (~80%). It has been speculated that hydrogen atom roaming may be most prevalent since hydrogen can more rapidly explore the potential energy surface.[5] However, more recent studies on acetaldehyde dissociation have shown that the methyl group was much more likely to roam than a hydrogen atom and accounts for an estimated 84 ± 10% of the products.[10] This observation was attributed to the near-isoenergetic thresholds for the CH_3 + HCO and the CH_4 + CO channels, a more favorable geometry for abstraction, and the ability of both the CH_3 and HCO fragments to couple excess reaction energy into the internal modes to prevent radical dissociation.[11] The molecular channel threshold for NO_3, like acetaldehyde, is nearly isoenergetic with the radical threshold.

The origin of the second pathway in NO_3 photodissoication, corresponding to low O_2 vibrational states, is unclear. We speculate that it arises either from a tight transition state not yet identified by theoretical calculations, the involvement of interactions with excited electronic states (such as the ^{2}E″),[12] or possibly a bifurcated roaming potential arising from oxygen abstraction at different NO_2 geometries. Further studies are required to interpret this unexpected behavior.

EXPERIMENTAL SECTION

The NO_3 precursor, N_2O_5, was synthesized by flowing ozone through a bubbler of trapped NO_2 at approximately −60 °C. The resulting N_2O_5 was then slowly trapped in a second bubbler at −78 °C, which crystallized as a white solid. A gas mixture of ~1% N_2O_5 was generated by flowing 800 Torr of He over the N_2O_5 sample placed in a −10 °C acetone bath. The N_2O_5 was converted to NO_3 by a flash pyrolytic source at 400−500 K.[13] The resulting expansion-cooled NO_3 was collimated by a conical skimmer into a molecular beam, which was intersected by two pulsed laser beams. The photolysis beam was generated by a Spectra Physics GCR-15-10 Nd:YAG (532 nm) pumped dye laser (PDL). Images were acquired at a variety of photolysis wavelengths above and below the product channel thresholds from 582 to 615 nm. The probe beam was generated by the THG of a second Nd:YAG laser (355 nm) pumping a LAS dye laser to generate 450 nm light, which was then frequency doubled to reach the 1 + 1 REMPI transitions of various NO rotational states in the 224−226 nm range. The resulting cations were accelerated by a set of electrostatic lenses down a 50 cm time-of-flight tube onto a position-sensitive microchannel plate phosphor assembly. The signal from this assembly was captured by a triggered CCD camera and sent to a computer for accumulation and analysis. The raw images were reconstructed to obtain velocity distributions using the POP (polar onion peeling) algorithm developed by Roberts et al.[14] The appearance of the NO_3 signal was shown to be dependent on the source temperature and photolysis wavelength and does not appear at ambient nozzle temperatures or when the photolysis laser is blocked. In addition, the intensity of the signal exhibited a wavelength dependence consistent with previous quantum yield measurements.

SUPPORTING INFORMATION AVAILABLE

A comparison between the total translational energy distribution obtained by ref 1 and a Boltzmann-weighted sum of the state-selected translational energy distributions of the current work. This material is available free of charge via the Internet at http://pubs.acs.org.

AUTHOR INFORMATION

Corresponding Author:

*To whom correspondence should be addressed. E-mail: swnorth@tamu.edu.

ACKNOWLEDGMENT

The authors would like to thank Wolfgang Eisfeld and H. Floyd Davis for helpful discussions regarding NO_3. We would also like to thank Justine Geidosch for her help in developing the synthesis of N_2O_5. Support for this project was provided by the Robert A. Welch Foundation (A-1405). A.G.S. further acknowledges the support of the Director, Office of Science, Office of Basic Energy Science, Division of Chemical Science, Geoscience and Bioscience, of the U.S. Department of Energy under Contract Number DE-FG02-04ER15593.

REFERENCES

(1) Davis, H. F.; Kim, B. S.; Johnston, H. S.; Lee, Y. T. Dissociation-Energy and Photochemistry of NO_3. *J. Phys. Chem.* **1993,** *97*, 2172.

(2) Magnotta, F.; Johnston, H. S. Photo-Dissociation Quantum Yields for the NO_3 Free-Radical. *Geophys. Res. Lett.* **1980,** *7*, 769.

(3) Orlando, J. J.; Tyndall, G. S.; Moortgat, G. K.; Calvert, J. G. Quantum Yields for NO_3 Photolysis between 570 and 635 nm. *J. Phys. Chem.* **1993,** *97*, 10996.

(4) Mikhaylichenko, K.; Riehn, C.; Valachovic, L.; Sanov, A.; Wittig, C. Unimolecular Decomposition of NO_3: The NO+O_2 Threshold Regime. *J. Chem. Phys.* **1996,** *105*, 6807.

(5) Townsend, D.; Lahankar, S. A.; Lee, S. K.; Chambreau, S. D.; Suits, A. G.; Zhang, X.; Rheinecker, J.; Harding, L. B.; Bowman,

DOI: 10.1021/jz1008888 | *J. Phys. Chem. Lett.* **2010,** *1*, 2455–2458

J. M. The Roaming Atom: Straying from the Reaction Path in Formaldehyde Decomposition. *Science* **2004,** *306*, 1158.
(6) Chen, C.; Braams, B.; Lee, D. Y.; Bowman, J. M.; Houston, P. L.; Stranges, D. Evidence for Vinylidene Production in the Photodissociation of the Allyl Radical. *J. Phys. Chem. Lett.* **2010,** *1*, 1875.
(7) Christoffel, K. M.; Bowman, J. M. Three Reaction Pathways in the H + HCO → H_2 + CO Reaction. *J. Phys. Chem. A* **2009,** *113*, 4138.
(8) Smith, I. W. M.; Tuckett, R. P.; Whitham, C. J. The Vibrational-State Distributions in Both Products of the Reaction −O-(^{3}P)+NO^{2-}]O_2+NO. *Chem. Phys. Lett.* **1992,** *200*, 615.
(9) Suits, A. G.; Chambreau, S. D.; Lahankar, S. A. State-Correlated DC Slice Imaging of Formaldehyde Photodissociation: Roaming Atoms and Multichannel Branching. *Int. Rev. Phys. Chem.* **2007,** *26*, 585.
(10) Heazlewood, B. R.; Jordan, M. J. T.; Kable, S. H.; Selby, T. M.; Osborn, D. L.; Shepler, B. C.; Braams, B. J.; Bowman, J. M. Roaming Is the Dominant Mechanism for Molecular Products in Acetaldehyde Photodissociation. *Proc. Natl. Acad. Sci. U.S. A.* **2008,** *105*, 12719.
(11) Houston, P. L.; Kable, S. H. Photodissociation of Acetaldehyde As a Second Example of the Roaming Mechanism. *Proc. Natl. Acad. Sci. U.S.A.* **2006,** *103*, 16079.
(12) Eisfeld, W.; Morokuma, K. Theoretical Study of the Potential Stability of the Peroxo Nitrate Radical. *J. Chem. Phys.* **2003,** *119*, 4682.
(13) Kim, H.; Dooley, K. S.; Johnson, E. R.; North, S. W. Design and Characterization of Late-Mixing Flash Pyrolytic Reactor Molecular-Beam Source. *Rev. Sci. Instrum.* **2005,** 76.
(14) Roberts, G. M.; Nixon, J. L.; Lecointre, J.; Wrede, E.; Verlet, J. R. R. Toward Real-Time Charged-Particle Image Reconstruction Using Polar Onion-Peeling. *Rev. Sci. Instrum.* **2009,** 80.

DOI: 10.1021/jz1008888 | *J. Phys. Chem. Lett.* **2010,** *1*, 2455–2458